

MESON PRODUCTION IN PROTON-PROTON COLLISIONS IN THE NAIVE NON-ABELIANIZATION APPROXIMATION AND THE ROLE OF INFRARED RENORMALONS

A. I. Ahmadov^{1,2} *, Sh. M. Nagiyev³, and E. A. Dadashov³

¹ *Department of Theoretical Physics, Baku State University*

Z. Khalilov Street 23, AZ-1148, Baku, Azerbaijan

² *TH Division, Physics Department, CERN*

CH-1211 Geneva 23, Switzerland and

³*Institute of Physics of Azerbaijan National Academy of Sciences,*

H. Javid Avenue, 33, AZ-1143, Baku, Azerbaijan

(Dated: June 14, 2018)

Abstract

We calculate the "naive non-abelianization" (NNA) contributions of the higher-twist Feynman diagrams to the large- p_T inclusive pion production cross section in proton-proton collisions in the case of the running coupling and frozen coupling approaches. We compare the resummed "naive non-abelianization" higher-twist cross sections with the ones obtained in the framework of the frozen coupling approach and leading-twist cross section. The structure of infrared renormalon singularities of the higher twist subprocess cross section and its resummed expression are found. We discuss the phenomenological consequences of possible higher-twist contributions to the pion production in proton-proton collisions in within NNA.

PACS numbers: 12.38.-t, 13.60.Le, 13.87.Fh, 14.40.Aq,

Keywords: higher-twist, naive non-abelianization, infrared renormalons

* ahmadovazar@yahoo.com

I. INTRODUCTION

The hadronic wave functions in terms of quark and gluon degrees of freedom play an important role in the quantum chromodynamics predictions for hadronic processes. If the hadronic wave functions were accurately known, then we could calculate the hadronic distribution amplitude and structure functions for exclusive and inclusive processes in quantum chromodynamics (QCD).

The large-order behavior of a perturbative expansion in gauge theories is inevitably dominated by the factorial growth of renormalon diagrams [1-4]. In the case of QCD, the coefficients of perturbative expansions in the QCD coupling α_s can increase dramatically even at low orders. This fact, together with the apparent freedom in the choice of renormalization scheme and renormalization scales, limits the predictive power of perturbative calculations, even in applications involving large momentum transfers, where α_s is effectively small. Investigation of the infrared renormalon effects in various inclusive and exclusive processes is one of the most important and interesting problem in the perturbative QCD (pQCD).

The frozen coupling constant approach in Refs.[5,6,7,8,9] was used for calculation of integrals, such as

$$I \sim \int \frac{\alpha_s(Q^2)\Phi(x, Q^2)}{1-x} dx \quad (1.1)$$

It should be noted that, in pQCD calculations, the argument Q^2 of the running coupling constant should be taken equal to the square of the momentum transfer of a hard gluon in a corresponding Feynman diagram, in both the renormalization and factorization scale. But defining in this way, $\alpha_s(Q^2)$ suffers from infrared singularities. Therefore, in the soft regions as $x_1 \rightarrow 0$, and $x_2 \rightarrow 0$, the integral in (1.1) diverge and we need some regularization methods for $\alpha_s(Q^2)$ in these regions for their calculation. It is known that infrared renormalons are responsible for factorial growth of coefficients in perturbative series for the physical quantities. But, these divergent series can be resummed by means of the Borel transformation [1] and the principal value prescription [10], and effects of infrared renormalons can be taken into account by a scale-setting procedure $\alpha_s(Q^2) \rightarrow \alpha_s(\exp(f(Q^2))Q^2)$ at the one-loop order results.

In this work we apply the running coupling approach [11] in order to compute the effects of the infrared renormalons on the meson production in proton-proton collisions in "naive non-abelianization" approximation. This approach was also employed previously [12-14]

to calculate the inclusive meson production in proton-proton and photon-photon collisions. The running coupling approach in "naive non-abelianization" approximation pion electromagnetic form factor was computed in [15].

A precise measurement of the inclusive charged pion production cross section at $\sqrt{s} = 62.4 \text{ GeV}$ and $\sqrt{s} = 200 \text{ GeV}$ is important for the proton-proton collisions program at the Relativistic Heavy Ion Collider (RHIC) at the Brookhaven National Laboratory.

Therefore, it will be interesting that the calculation of the higher-twist effects on the dependence of the pion wave function in pion production at proton-proton collisions by the running coupling constant approach. In this respect, the contribution of the higher-twist Feynman diagrams to a pion production cross section in proton-proton collisions has been computed by using the the infrared renormalon improved distribution amplitude of the pion. Also, higher-twist contributions which are calculated by the running coupling constant and frozen coupling constant approaches are been estimated and compared to each other. Within this context, this paper is organized as follows: In Sec. II, we provide formulas for the calculation of the contribution of the higher twist and leading twist diagrams. In Sec. III we present formulas and an analysis of the higher-twist effects on the dependence of the pion wave function by the running coupling constant approach. In Sec. IV, we give the numerical results for the cross section and discuss the dependence of the cross section on the pion wave functions. We present our conclusions in Sec. V.

II. THE HIGHER TWIST AND LEADING TWIST CONTRIBUTIONS TO INCLUSIVE REACTIONS

The higher-twist Feynman diagrams, which describe the subprocess $q_1 + \bar{q}_2 \rightarrow \pi^+(\pi^-) + \gamma$ for the pion production in the proton-proton collision are shown in Fig.1. The amplitude for this subprocess can be found by means of the Brodsky-Lepage formula [16]:

$$M(\hat{s}, \hat{t}) = \int_0^1 dx_1 \int_0^1 dx_2 \delta(1 - x_1 - x_2) \Phi_\pi(x_1, x_2, Q^2) T_H(\hat{s}, \hat{t}; x_1, x_2). \quad (2.1)$$

In Eq.(2.1), T_H is the sum of the graphs contributing to the hard-scattering part of the subprocess. In our calculation, we have neglected the pion and the proton masses. The Mandelstam invariant variables for subprocesses $q_1 + \bar{q}_2 \rightarrow \pi^+(\pi^-) + \gamma$ are defined as

$$\hat{s} = (p_1 + p_2)^2, \quad \hat{t} = (p_1 - p_\pi)^2, \quad \hat{u} = (p_1 - p_\gamma)^2. \quad (2.2)$$

One of the important moment in our study is the choice of the pion wave functions $\Phi_\pi(x, Q^2)$ in Eq.(2.1). In Ref.[16] the authors have calculated the contribution of "bubble chain" diagrams to the Brodsky-Lepage evolution kernel $V[x, y; \alpha(Q^2)]$ in the "naive non-abelianization" (NNA) approximation and, as a result, have got new, infrared renormalon improved distribution amplitude for the meson in the form:

$$\Phi_\pi(x, Q^2) = f_M[x(1-x)]^{1+\alpha} \sum_{n=0}^{\infty} a_n(Q^2) A_n C_n^{3/2+\alpha}(2x-1) \quad (2.3)$$

where $C_n^{3/2+\alpha}(2x-1)$ are the Gegenbauer polynomials, $A_n(\alpha_s)$ are normalization constants, $a_n(Q^2)$ define the evolution of $\Phi_\pi(x, Q^2)$ with Q^2 and $\alpha \equiv \alpha_s(Q^2)\beta_0/4\pi$. In our calculations are normalization constants $A_n(\alpha_s)$ are given by the expression

$$A_n(\alpha_s) = \frac{\Gamma(3+2\alpha)}{\sqrt{3}\Gamma(1+\alpha)\Gamma(2+\alpha)} \cdot \frac{n!}{(2+2\alpha)_n} \cdot \frac{3+2\alpha+2n}{2+2\alpha+n}. \quad (2.4)$$

where $\Gamma(a)$ is the Euler gamma function, $(a)_n$ is the Pochhammer symbol, $(a)_n = \Gamma(a+n)/\Gamma(a)$. It should be noted that normalization constants $A_n(\alpha_s)$ given by expression (2.4) differ from ones of Ref.[17]. If in the Ref.[17] change α by $\alpha+1$, then we obtain expression (2.4). We have used three different wave functions: the asymptotic (asy), and the Gosdzinsky-Kivel wave functions [17].

$$\begin{aligned} \Phi_{GK1}(x, \mu_0^2) &= \Phi_{asy}(x, \alpha) \left[C_0^{3/2+\alpha}(2x-1) + 1.7A_2C_2^{3/2+\alpha}(2x-1) \right], \\ \Phi_{GK2}(x, \mu_0^2) &= \Phi_{asy}(x, \alpha) \left[C_0^{3/2+\alpha}(2x-1) + 1.7A_2C_2^{3/2+\alpha}(2x-1) + 1.6A_4C_4^{3/2+\alpha}(2x-1) \right], \\ \Phi_{asy}(x, \alpha) &= f_\pi \frac{\Gamma(4+2\alpha)}{2\Gamma^2(2+\alpha)} [x(1-x)]^{1+\alpha}, \end{aligned} \quad (2.5)$$

$$\begin{aligned} C_0^{3/2+\alpha}(2x-1) &= 1, \quad C_2^{3/2+\alpha}(2x-1) = \frac{3+2\alpha}{2}((5+2\alpha)(2x-1)^2 - 1), \\ C_4^{3/2+\alpha}(2x-1) &= \frac{(3+2\alpha)(5+2\alpha)}{24}[(9+2\alpha)(7+2\alpha)(2x-1)^4 - 6(7+2\alpha)(2x-1)^2 + 3] \end{aligned}$$

where f_π is the pion decay constant. The evolution of the wave function on the factorization scale Q^2 is governed by the functions $a_n(Q^2)$,

$$a_n(Q^2) = a_n(\mu_0^2) \exp \left[\int_{\alpha_s(\mu_0^2)}^{\alpha_s(p_T^2)} 4\pi \frac{\gamma_k(x) + C_{kk}(x)}{\beta_0 x^2} dx \right], \quad (2.6)$$

where

$$C_{kk}(\alpha_s) = (\alpha_s \frac{\beta_0}{4\pi})^2 \left\{ \psi\left(\frac{3}{2} + \alpha + 2k\right) - \psi\left(\frac{3}{2} + \alpha\right) \right\}, \quad (2.7)$$

$$\gamma_n = C_F \frac{(1+\alpha)^2 \Gamma(2\alpha+4)}{3(2+\alpha) \Gamma(2+\alpha)^3 \Gamma(1-\alpha)} \left\{ 1 - \frac{(\alpha+1)(\alpha+2)}{(\alpha+1+n)(\alpha+n+2)} + \frac{2(\alpha+2)}{\alpha+1} [\psi(\alpha+2+n) - \psi(\alpha+2)] \right\}. \quad (2.8)$$

In the limit $\alpha \rightarrow 0$ from infrared renormalon improved distribution amplitude we can obtain ordinary distribution amplitude.

The cross section for the higher-twist subprocess $q_1 \bar{q}_2 \rightarrow \pi^+(\pi^-)\gamma$ is given by the expression

$$\frac{d\sigma}{d\hat{t}}(\hat{s}, \hat{t}, \hat{u}) = \frac{8\pi^2 \alpha_E C_F}{27} \frac{[D(\hat{t}, \hat{u})]^2}{\hat{s}^3} \left[\frac{1}{\hat{u}^2} + \frac{1}{\hat{t}^2} \right], \quad (2.9)$$

where

$$D(\hat{t}, \hat{u}) = e_1 \hat{t} \int_0^1 dx \left[\frac{\alpha_s(Q_1^2) \Phi_\pi(x, Q_1^2)}{1-x} \right] + e_2 \hat{u} \int_0^1 dx \left[\frac{\alpha_s(Q_2^2) \Phi_\pi(x, Q_2^2)}{1-x} \right]. \quad (2.10)$$

Here $Q_1^2 = (x-1)\hat{u}$, and $Q_2^2 = -x\hat{t}$, represent the momentum squared carried by the hard gluon in Fig.1, $e_1(e_2)$ is the charge of $q_1(\bar{q}_2)$ and $C_F = \frac{4}{3}$. The higher-twist contribution to the large- p_T pion production cross section in the process $pp \rightarrow \pi^+(\pi^-) + \gamma + X$ is [18,19]:

$$\Sigma_M^{HT} \equiv E \frac{d\sigma}{d^3p} = \int_0^1 \int_0^1 dx_1 dx_2 G_{q_1/h_1}(x_1) G_{q_2/h_2}(x_2) \frac{\hat{s}}{\pi} \frac{d\sigma}{d\hat{t}}(q\bar{q} \rightarrow \pi\gamma) \delta(\hat{s} + \hat{t} + \hat{u}). \quad (2.11)$$

In the numerical calculations we denote the higher-twist cross section obtained using the frozen coupling constant approximation by $(\Sigma_\pi^{HT})^0$.

One of the essential problem, extracting the higher-twist corrections to the pion production cross section and a comparison of higher-twist corrections with leading-twist contributions. We take two leading-twist subprocesses for the pion production: (1) quark-antiquark annihilation $q\bar{q} \rightarrow g\gamma$, in which $g \rightarrow \pi^+(\pi^-)$ and (2) quark-gluon fusion, $qg \rightarrow q\gamma$, with subsequent fragmentation of the final quark into a meson, $q \rightarrow \pi^+(\pi^-)$.

III. HIGHER-TWIST MECHANISM AND THE ROLE OF INFRARED RENORMALONS

In this section, we will calculate the integral (2.10) using the running coupling constant approach in the naive non-abelianization approximation and also discuss the problem of normalization of the higher-twist process cross section in the context of the same approach. As is seen from (2.10), in general, one has to take into account not only the dependence of $\alpha(Q^2)$ on the scale Q^2 , but also an evolution of $\Phi(x, Q^2)$ with Q^2 . Therefore, it is worth

noting that, the renormalization scale (argument of α_s) should be equal to $Q_1^2 = (x-1)\hat{u}$, $Q_2^2 = -x\hat{t}$, whereas the factorization scale [Q^2 in $\Phi_M(x, Q^2)$] is taken independent from x , we assume $Q^2 = p_T^2$. It should be noted in Ref.[17] the authors also noted the existence of two kinds of power corrections to cross sections; the infrared renormalon ambiguity arising from the loop integration and power corrections from regions as, $x \rightarrow 0$, $x \rightarrow 1$. The integral (2.10) in the framework of the running coupling approach takes the form

$$I(\mu_{R_0}^2) = \int_0^1 \frac{\alpha_s(\lambda\mu_{R_0}^2)\Phi_M(x, \mu_F^2)dx}{1-x}. \quad (3.1)$$

The $\alpha_s(\lambda\mu_{R_0}^2)$ has the infrared singularity at $x \rightarrow 1$, for $\lambda = 1-x$ or $x \rightarrow 0$, for $\lambda = x$ and so the integral (3.1) diverges. Hence, the integral (3.1) can be found after regularization of $\alpha_s(\lambda\mu_{R_0}^2)$ in these end point regions. Such regularization can be fulfilled with the aid of the renormalization group equation that allows us to express the running coupling constant $\alpha_s(\lambda Q^2)$ in terms of $\alpha_s(Q^2)$. The solution of renormalization group equation for the running coupling $\alpha \equiv \alpha_s/\pi$ has the form [10]

$$\frac{\alpha(\lambda)}{\alpha} = \left[1 + \alpha \frac{\beta_0}{4} \ln \lambda\right]^{-1}. \quad (3.2)$$

Then for $\alpha(\lambda Q^2)$, we get

$$\alpha(\lambda Q^2) = \frac{\alpha_s}{1 + \ln \lambda/t}. \quad (3.3)$$

where $t = 4\pi/\alpha_s(Q^2)\beta_0 = 4/\alpha\beta_0$.

Having inserted Eq.(3.3) into Eq.(2.10) we obtain

$$\begin{aligned} D(\hat{t}, \hat{u}) = & e_1 \hat{t} \alpha_s(-\hat{u}) t_1 \int_0^1 dx \frac{f_M[x(1-x)]^{1+\alpha} \sum_{n=0}^{\infty} a_n(Q^2) A_n C_n^{3/2+\alpha} (2x-1)}{(1-x)(t_1 + \ln \lambda)} + \\ & e_2 \hat{u} \alpha_s(-\hat{t}) t_2 \int_0^1 dx \frac{f_M[x(1-x)]^{1+\alpha} \sum_{n=0}^{\infty} a_n(Q^2) A_n C_n^{3/2+\alpha} (2x-1)}{(1-x)(t_2 + \ln \lambda)} \end{aligned} \quad (3.4)$$

where $t_1 = 4\pi/\alpha_s(-\hat{u})\beta_0$ and $t_2 = 4\pi/\alpha_s(-\hat{t})\beta_0$.

The integral (3.4) as we know, still divergent, which can be defined by existing methods. Using the running coupling approach it may be found as a perturbative series in $\alpha_s(Q^2)$ with factorially growing coefficient. Making the change variable as $z = \ln \lambda$ we obtain

$$D(\hat{t}, \hat{u}) = e_1 \hat{t} \alpha_s(-\hat{u}) t_1 \int_0^1 dx \frac{\Phi_M(x, p_T^2)}{(1-x)(t_1 + z)} + e_2 \hat{u} \alpha_s(-\hat{t}) t_2 \int_0^1 dx \frac{\Phi_M(x, p_T^2)}{(1-x)(t_2 + z)} \quad (3.5)$$

In order to calculate (3.5) we will apply the integral representation of $1/(t+z)$ [20,21].

$$\frac{1}{(t+z)} = \int_0^{\infty} e^{-(t+z)u} du \quad (3.6)$$

gives

$$D(\hat{t}, \hat{u}) = e_1 \hat{t} \alpha_s(-\hat{u}) t_1 \int_0^1 \int_0^\infty \frac{\Phi_M(x, p_T^2) e^{-(t_1+z)u} du dx}{(1-x)} + \\ e_2 \hat{u} \alpha_s(-\hat{t}) t_2 \int_0^1 \int_0^\infty \frac{\Phi_M(x, p_T^2) e^{-(t_2+z)u} du dx}{(1-x)}. \quad (3.7)$$

In the case $\Phi_{asy}(x, \alpha)$ for the $D(\hat{t}, \hat{u})$, it is written as

$$D(\hat{t}, \hat{u}) = \frac{4\pi f_\pi e_1 \hat{t}}{\beta_0} \cdot \frac{\Gamma(4+2\alpha)}{2\sqrt{3}\Gamma^2(2+\alpha)} \cdot \int_0^\infty du e^{-t_1 u} B(2+\alpha, 1+\alpha-u) + \\ \frac{4\pi f_\pi e_2 \hat{u}}{\beta_0} \cdot \frac{\Gamma(4+2\alpha)}{2\sqrt{3}\Gamma^2(2+\alpha)} \cdot \int_0^\infty du e^{-t_2 u} B(2+\alpha, 1+\alpha-u). \quad (3.8)$$

and for $\Phi_{GK1}(x, Q^2)$ wave function

$$D(\hat{t}, \hat{u}) = \frac{4\pi f_\pi e_1 \hat{t}}{\beta_0} \cdot \frac{\Gamma(4+2\alpha)}{2\sqrt{3}\Gamma^2(2+\alpha)} \cdot \int_0^\infty du e^{-t_1 u} [A_0(\alpha_s) B(2+\alpha, 1+\alpha-u) + 1.7 A_2(\alpha_s) \frac{3+2\alpha}{2} \cdot \\ \exp\left(\frac{4\pi}{\beta_0} \int_{\alpha_s(\mu_0^2)}^{\alpha_s(p_T^2)} \frac{\gamma_k(x) + C_{kk}(x)}{x^2} dx\right) ((5+2\alpha)(4B(4+\alpha, 1+\alpha-u) - \\ 4B(3+\alpha, 1+\alpha-u) + B(2+\alpha, 1+\alpha-u)) - B(2+\alpha, 1+\alpha-u)] + \\ \frac{4\pi f_\pi e_2 \hat{u}}{\beta_0} \cdot \frac{\Gamma(4+2\alpha)}{2\sqrt{3}\Gamma^2(2+\alpha)} \cdot \int_0^\infty du e^{-t_2 u} [A_0(\alpha_s) B(2+\alpha, 1+\alpha-u) + 1.7 A_2(\alpha_s) \frac{3+2\alpha}{2} \cdot \\ \exp\left(\frac{4\pi}{\beta_0} \int_{\alpha_s(\mu_0^2)}^{\alpha_s(p_T^2)} \frac{\gamma_k(x) + C_{kk}(x)}{x^2} dx\right) ((5+2\alpha)(4B(4+\alpha, 1+\alpha-u) - \\ 4B(3+\alpha, 1+\alpha-u) + B(2+\alpha, 1+\alpha-u)) - B(2+\alpha, 1+\alpha-u)]. \quad (3.9)$$

also for $\Phi_{GK2}(x, Q^2)$ wave function

$$D(\hat{t}, \hat{u}) = \frac{4\pi f_\pi e_1 \hat{t}}{\beta_0} \cdot \frac{\Gamma(4+2\alpha)}{2\sqrt{3}\Gamma^2(2+\alpha)} \cdot \int_0^\infty du e^{-t_1 u} [A_0(\alpha_s) B(2+\alpha, 1+\alpha-u) + 1.7 A_2(\alpha_s) \frac{3+2\alpha}{2} \cdot \\ \exp\left(\frac{4\pi}{\beta_0} \int_{\alpha_s(\mu_0^2)}^{\alpha_s(p_T^2)} \frac{\gamma_k(x) + C_{kk}(x)}{x^2} dx\right) ((5+2\alpha)(4B(4+\alpha, 1+\alpha-u) - \\ 4B(3+\alpha, 1+\alpha-u) + B(2+\alpha, 1+\alpha-u)) - B(2+\alpha, 1+\alpha-u)] + \\ 1.6 A_4(\alpha_s) \frac{(3+2\alpha)(5+2\alpha)}{24} \cdot \\ \exp\left(\frac{4\pi}{\beta_0} \int_{\alpha_s(\mu_0^2)}^{\alpha_s(p_T^2)} \frac{\gamma_k(x) + C_{kk}(x)}{x^2} dx\right) ((9+2\alpha)(7+2\alpha)(16B(6+\alpha, 1+\alpha-u) - \\ 32B(5+\alpha, 1+\alpha-u) + 24B(4+\alpha, 1+\alpha-u) - 8B(3+\alpha, 1+\alpha-u) + B(2+\alpha, 1+\alpha-u)) -$$

$$\begin{aligned}
& 6(7+2\alpha)(4B(4+\alpha, 1+\alpha-u)- \\
& 4B(3+\alpha, 1+\alpha-u) + B(2+\alpha, 1+\alpha-u)) + 3B(2+\alpha, 1+\alpha-u)] + \\
& \frac{4\pi f_\pi e_2 \hat{u}}{\beta_0} \cdot \frac{\Gamma(4+2\alpha)}{2\sqrt{3}\Gamma^2(2+\alpha)} \cdot \int_0^\infty du e^{-t_2 u} [A_0(\alpha_s)B(2+\alpha, 1+\alpha-u) + 1.7A_2(\alpha_s)\frac{3+2\alpha}{2} \cdot \\
& \exp\left(\frac{4\pi}{\beta_0} \int_{\alpha_s(\mu_0^2)}^{\alpha_s(p_T^2)} \frac{\gamma_k(x) + C_{kk}(x)}{x^2} dx\right) \left((5+2\alpha)(4B(4+\alpha, 1+\alpha-u)- \right. \\
& 4B(3+\alpha, 1+\alpha-u) + B(2+\alpha, 1+\alpha-u)) - B(2+\alpha, 1+\alpha-u)] + \\
& 1.6A_4(\alpha_s)\frac{(3+2\alpha)(5+2\alpha)}{24} \cdot \\
& \exp\left(\frac{4\pi}{\beta_0} \int_{\alpha_s(\mu_0^2)}^{\alpha_s(p_T^2)} \frac{\gamma_k(x) + C_{kk}(x)}{x^2} dx\right) ((9+2\alpha)(7+2\alpha)(16B(6+\alpha, 1+\alpha-u)- \\
& 32B(5+\alpha, 1+\alpha-u) + 24B(4+\alpha, 1+\alpha-u) - 8B(3+\alpha, 1+\alpha-u) + B(2+\alpha, 1+\alpha-u)) - \\
& 6(7+2\alpha)(4B(4+\alpha, 1+\alpha-u)- \\
& 4B(3+\alpha, 1+\alpha-u) + B(2+\alpha, 1+\alpha-u)) + 3B(2+\alpha, 1+\alpha-u)]. \tag{3.10}
\end{aligned}$$

where $B(\alpha, \beta)$ is Beta function.

The inverse Borel transformations have the infinite number of infrared renormalon poles at the points $u_0 = k + \alpha$ in the Borel plane. According to Ref.[4] that infrared renormalon pole at $u_0 = k$ correspond to a power-suppressed correction as $(\Lambda^2/Q^2)^k$ to a physical quantity under consideration. If the renormalon pole is located at $u_0 = k + \alpha$ then its contribution is order $(\Lambda^2/Q^2)^k/e$ or $(\Lambda^2/Q^2)^k/e^2$. Therefore, our expressions (3.8)-(3.10) takes into account the power-suppressed corrections $C_k(Q^2)(\Lambda^2/Q^2)^k$, $k = 1, 2, 3, ..$ to the inclusive pion production cross section in proton-proton collisions. The coefficients $C_k(Q^2)$ of these corrections also depend on the chosen pion wave functions. It should be noted that here we neglect infrared ambiguities $\delta C_k(Q^2)(\Lambda^2/Q^2)^k$ producing by the principal value prescription itself, which have to be canceled by ultraviolet renormalon ambiguities of higher twist corrections to cross section and do not estimate $\delta C_k(Q^2)$. The structure of the infrared renormalon poles in Eqs.(3.8-3.10) strongly depends on the wave functions of the pion. In the numerical calculations we denote resummed higher-twist cross section by $(\Sigma_\pi^{HT})^{res}$.

IV. NUMERICAL RESULTS AND DISCUSSION

In this section, the numerical results for the "naive non-abelianization" contribution of higher-twist effects to large- p_T inclusive pion production cross section in the process $pp \rightarrow \pi^+ (or \pi^-) \gamma + X$ in the case higher-twist contributions calculated in the context of the running coupling and frozen coupling approaches on the dependence of the infrared renormalon improved distribution amplitude of the pion are discussed. In the numerical calculations for the quark distribution function inside the proton, the MSTW distribution function has been used [22]. The gluon and quark fragmentation functions into a pion has been taken from [23]. The results of our numerical calculations are plotted in Fig.2- Fig.9. In Fig.2 - Fig.4 we show the dependence of the higher-twist cross sections $(\Sigma_{\pi^+}^{HT})^0$, $(\Sigma_{\pi^+}^{HT})^{res}$ calculated in the context of the frozen and running couplings constant approaches and the ratios $R = (\Sigma_{\pi^+}^{HT})^{res}/(\Sigma_{\pi^+}^{HT})^0$, $(\Sigma_{\pi^+}^{HT})^0/(\Sigma_{\pi^+}^{LT})$, $(\Sigma_{\pi^+}^{HT})^{res}/(\Sigma_{\pi^+}^{LT})$ as a function of the pion transverse momentum p_T for different pion wave functions at $y = 0$. It is seen from Fig.2 that the higher-twist cross section is monotonically decreasing with an increase in the transverse momentum of the pion. In Fig.3 - Fig.4, we show the dependence of the ratios $R = (\Sigma_{\pi^+}^{HT})^{res}/(\Sigma_{\pi^+}^{HT})^0$, $(\Sigma_{\pi^+}^{HT})^0/\Sigma_{\pi^+}^{LT}$, $(\Sigma_{\pi^+}^{HT})^{res}/\Sigma_{\pi^+}^{LT}$ as a function of the pion transverse momentum p_T for different pion wave functions. Here $\Sigma_{\pi^+}^{LT}$ is the leading-twist cross section, respectively. As shown in Fig.3, in the region $2 \text{ GeV}/c < p_T < 4 \text{ GeV}/c$ resummed higher-twist cross section is suppress by about 1-2 orders of magnitude relative to the higher-twist cross section calculated in the framework of the frozen coupling approach. In Fig.4, we show the dependence of the ratios $(\Sigma_{\pi^+}^{HT})^0/\Sigma_{\pi^+}^{LT}$, and $(\Sigma_{\pi^+}^{HT})^{res}/\Sigma_{\pi^+}^{LT}$ as a function of the pion transverse momentum p_T for different pion wave functions. It is observed from Fig.4 that, the ratio $(\Sigma_{\pi^+}^{HT})^0/\Sigma_{\pi^+}^{LT}$ with increasing transverse momentum of pion decrease and has a minimum approximately at the point $p_T = 10 \text{ GeV}/c$. After that, the ratio increase with increasing in the p_T transverse momentum of the pion. Also, as shown in Fig.4, the ratio $(\Sigma_{\pi^+}^{HT})^{res}/\Sigma_{\pi^+}^{LT}$ decrease with increasing in the p_T transverse momentum of the pion. In Fig.5, we have depicted higher-twist cross sections $(\Sigma_{\pi^+}^{HT})^0$, $(\Sigma_{\pi^+}^{HT})^{res}$, as a function of the rapidity y of the pion at $\sqrt{s} = 62.4 \text{ GeV}$ and $p_T = 4.9 \text{ GeV}/c$. Figure show that higher-twist cross section in case frozen and running coupling constant approaches have a different distinctive. In the region $(-2.52 \leq y \leq 1.22)$ the higher-twist cross section $(\Sigma_{\pi^+}^{HT})^0$ for all wave functions increase with an increase of the y rapidity of the pion and

has a maximum approximately at the point $y = 1.22$. But, the resummed higher-twist cross section $(\Sigma_{\pi^+}^{HT})^{res}$ for all wave functions increase with an increase of the y rapidity of the pion and has a maximum approximately at the point $y = -1.92$. As is seen from Fig.5 in the region $-2.52 \leq y \leq 2$ resummed higher-twist cross section for $\Phi_{GK1}(x, Q^2)$ and $\Phi_{GK2}(x, Q^2)$ is suppressed by about one order of magnitude relative to the resummed higher-twist cross section for $\Phi_{asy}(x, \alpha)$. As is seen from Fig.6 ratio $R = (\Sigma_{\pi^+}^{HT})^{res}/(\Sigma_{\pi^+}^{HT})^0$, for all wave functions increase with an increase of the y rapidity of the pion and has a maximum approximately at the point $y = -1.92$. In the region $-2.52 < y < -1.92$ resummed higher-twist cross section is suppress by about two orders of magnitude relative to the higher-twist cross section calculated in the framework of the frozen coupling approach. Besides that, the ratio decreases with an increase in the y rapidity of the pion. Analysis of our calculations shows that $(\Sigma_{\pi^+}^{HT})^0$, $(\Sigma_{\pi^+}^{HT})^{res}$ higher-twist cross sections are sensitive to the choice of the infrared renormalon improved distribution amplitude of the pion. We have also carried out comparative calculations in the center-of-mass energy $\sqrt{s} = 200 \text{ GeV}$ and obtained results are displayed in Fig.7-Fig9. Analysis of our calculations at the center-of-mass energies $\sqrt{s} = 62.4 \text{ GeV}$ and $\sqrt{s} = 200 \text{ GeV}$, show that the increasing in the beam energy contributions of higher twist effects to the cross section decrease by about one-two order. In our calculations of the higher-twist cross section of the process the dependence of the transverse momentum of pion appears in the range of $(10^{-8} - 10^{-26})mb/GeV^2$. We think, that higher-twist cross section obtained in this work should be observable at RHIC.

V. CONCLUSIONS

Proton-proton collisions are known to be the most elementary interactions and form the very basis of our knowledge about the nature of high energy collisions in general. Physicists, by and large, hold the view quite firmly that the perturbative quantum-chromodynamics provides a general framework for the studies on high energy particle-particle collisions. Obviously, the unprecedented high energies attained at Large Hadron Collider offer new window and opportunities to test the proposed QCD dynamics with its pros and cons. However, we should remember that LHC opens a new kinematical regime at high energy, where several questions related to the description of the high-energy regime of the QCD. Consequently, studies of proton-proton interactions at the RHIC and LHC could provide valuable infor-

mation on the QCD dynamics at high energies. In this work the "naive non-abelianization" (NNA) contributions of the higher-twist Feynman diagrams to the large- p_T inclusive pion production cross section in proton-proton collisions are calculated. For calculation of the higher-twist cross section the running coupling constant approach is applied and infrared renormalon poles in the cross section expression are revealed. Infrared renormalon induced divergences is regularized by the means of the principal value prescription and the resummed expression (the Borel sum) for the higher-twist cross section is found. It is observed that, the resummed higher-twist cross section differs from that found using the frozen coupling approach, in some regions, considerably. Also we have demonstrated that higher-twist contributions to pion production cross section in the proton-proton collisions have important phenomenological consequences. Future RHIC and LHC measurements will provide further tests of the dynamics of large p_T hadron production beyond leading twist.

Acknowledgments

The work presented in this paper was started while one of the authors, A.I.Ahmadov, was visiting the TH Division of the CERN. He would like to express his gratitude to the members of the TH Division especially to the Prof. Jonathan Ellis for their hospitality. A.Ahmadov is also grateful to Stanley J.Brodsky for useful discussions. Financial support by CERN is also gratefully acknowledged.

VI. REFERENCES

- [1] G.'t. Hooft, in *The Whys of Subnuclear Physics*, Erice, 1977, edited by A. Zichichi (Plenum, New York, 1979), p.94
- [2] A. H. Mueller, *Nucl. Phys.* **B250**, 327 (1985); *Phys. Lett.* **B308**, 355 (1993).
- [3] V. I. Zakharov, *Nucl. Phys.* **B385**, 452 (1992).
- [4] M. Beneke, *Phys. Rep.* **317**, 1 (1999).
- [5] J. A. Bagger and J. F. Gunion, *Phys. Rev.* **D25**, 2287 (1982).
- [6] V. N. Baier and A. Grozin, *Phys. Lett.* **B96**, 181 (1980).
- [7] S. Gupta, *Phys. Rev.* **D24**, 1169 (1981).

- [8] A. I. Ahmadov, I. Boztosun, R. Kh. Muradov, A. Soylu and E. A. Dadashov, Int. J. Mod. Phys. **E15**, 1209 (2006).
- [9] A. I. Ahmadov, I. Boztosun, A. Soylu, and E. A. Dadashov, Int. J. Mod.Phys. **E17**, 1041 (2008).
- [10] H. Contopanagos and G. Sterman, Nucl. Phys. **B419**, 77 (1994).
- [11] S. S. Agaev, Phys. Lett. **B360**, 117 (1995); **B369**, 379(E) (1996).
- [12] A. I. Ahmadov, Coskun Aydin, Sh. M. Nagiyev, Yilmaz A. Hakan, and E. A. Dadashov, Phys. Rev. **D80**, 016003 (2009).
- [13] A. I. Ahmadov, Coskun Aydin, E. A. Dadashov and Sh. M. Nagiyev, Phys. Rev. **D81**, 054016 (2010).
- [14] A. I. Ahmadov, R. M. Burjaliyev, Int. J. Mod. Phys. **E20**, 1243 (2011).
- [15] S. S. Agaev, Modern Physics Letters **A15**, 1419 (2000).
- [16] G. L. Lepage and S. J. Brodsky, Phys. Rev. **D22**, 2157 (1980).
- [17] P. Gosdzinsky and N. Kivel, Nucl.Phys.**B521**, 274 (1998).
- [18] J. F. Owens, Rev. Mod. Phys. **59**, 465 (1987).
- [19] W. Greiner, S. Schramm and E. Stein, Quantum Chromodynamics, 2nd edn.(Berlin, Springer, 2002), pp.551.
- [20] J. Zinn-Justin, Phys. Rept. **70**, 109 (1981).
- [21] A. Erdelyi, Higher Transcendental Functions (McGrow-HillBook Company, New York, 1953), Vol.2.
- [22] A. D. Martin, W. J. Stirling, R. S. Thorne, and G. Watt, hep-ph/0901.0002.
- [23] S. Albino, B. A. Kniehl, G. Kramer, Nucl. Phys. **B725**, 181 (2005).

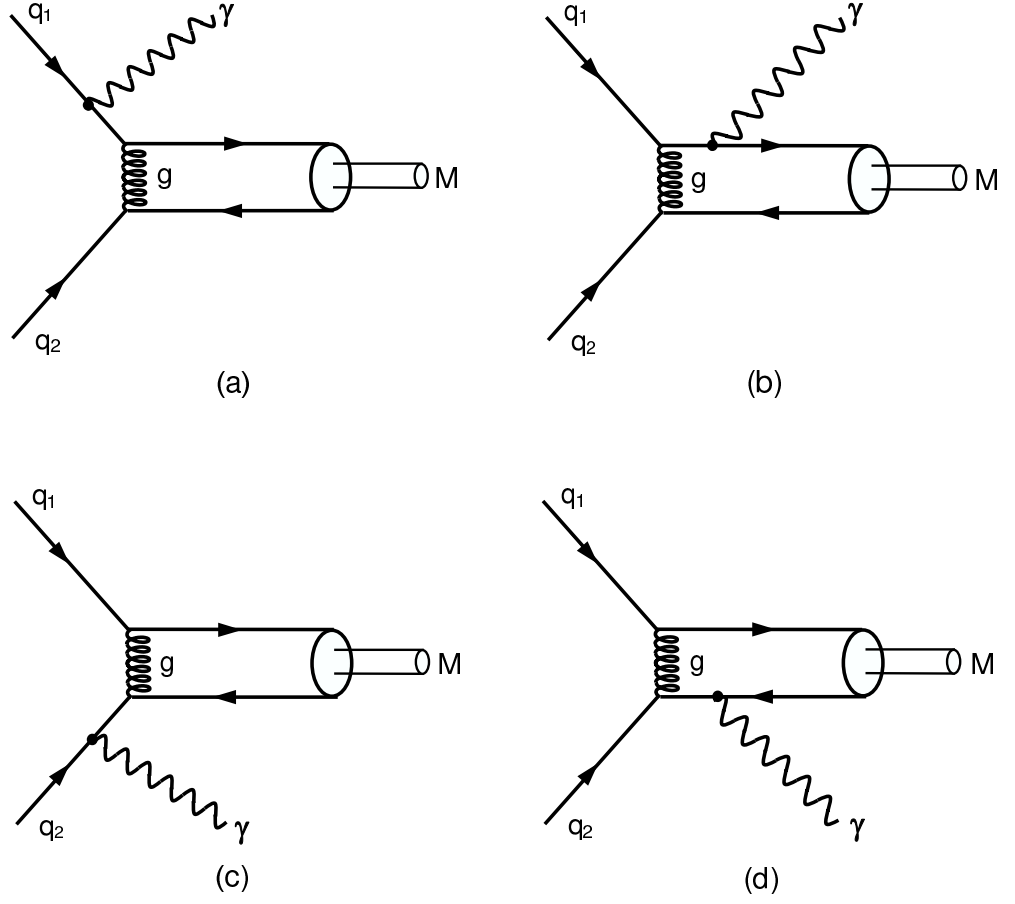


FIG. 1: Feynman diagrams for the higher-twist subprocess, $q_1 q_2 \rightarrow \pi^+ (\text{or } \pi^-) \gamma$.

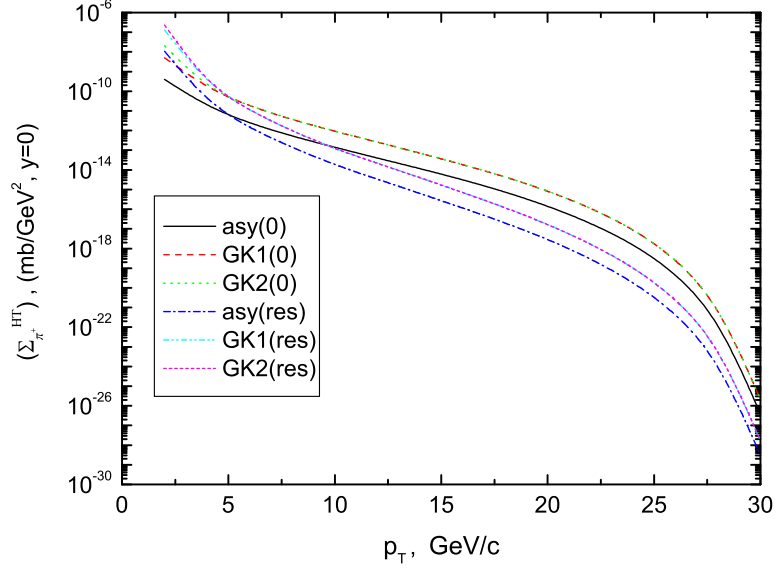


FIG. 2: Higher-twist π^+ production cross section $(\Sigma_{\pi^+}^{HT})$ as a function of the p_T transverse momentum of the pion at the c.m.energy $\sqrt{s} = 62.4 \text{ GeV}$.

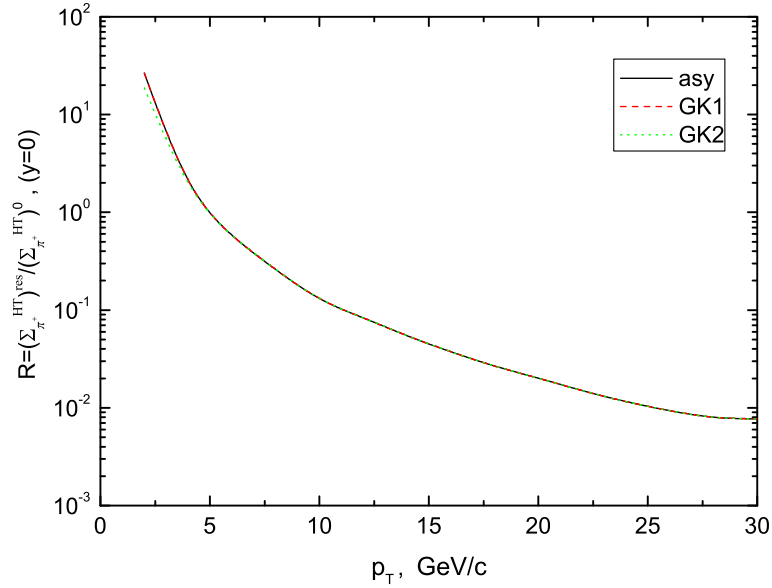


FIG. 3: Ratio $R = (\Sigma_{\pi^+}^{HT})^{res}/(\Sigma_{\pi^+}^{HT})^0$, where higher-twist contribution are calculated for the pion rapidity $y = 0$ at the c.m.energy $\sqrt{s} = 62.4 \text{ GeV}$ as a function of the pion transverse momentum, p_T .

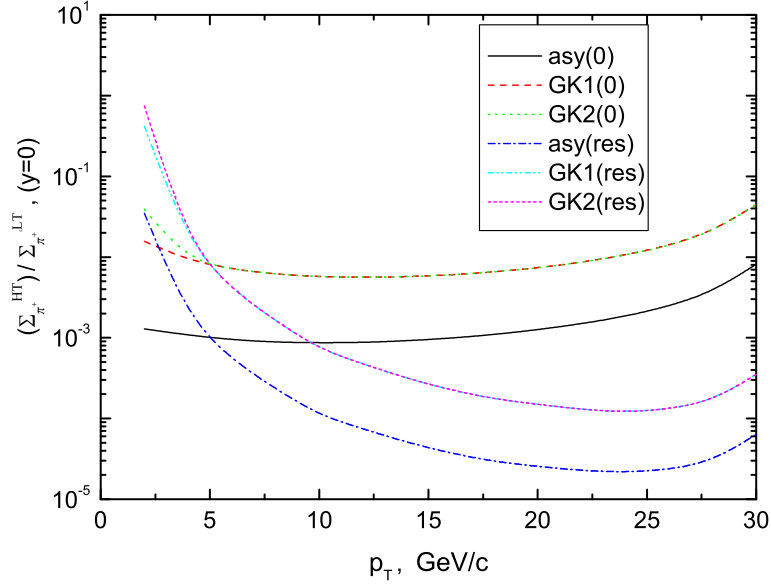


FIG. 4: Ratio $(\Sigma_{\pi^+}^{HT})/\Sigma_{\pi^+}^{LT}$, as a function of the p_T transverse momentum of the pion at the c.m.energy $\sqrt{s} = 62.4 \text{ GeV}$.

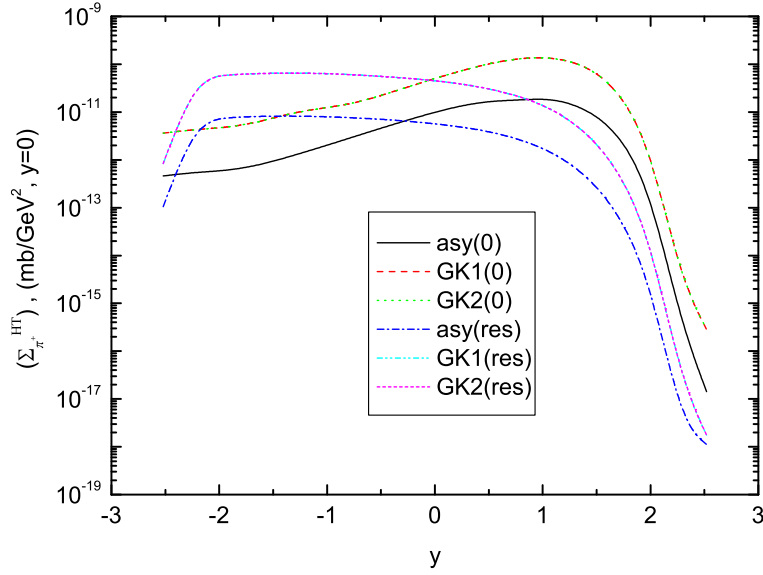


FIG. 5: Higher-twist π^+ production cross section $(\Sigma_{\pi^+}^{HT})$, as a function of the y rapidity of the pion at the transverse momentum of the pion $p_T = 4.9 \text{ GeV}/c$, at the c.m. energy $\sqrt{s} = 62.4 \text{ GeV}$.

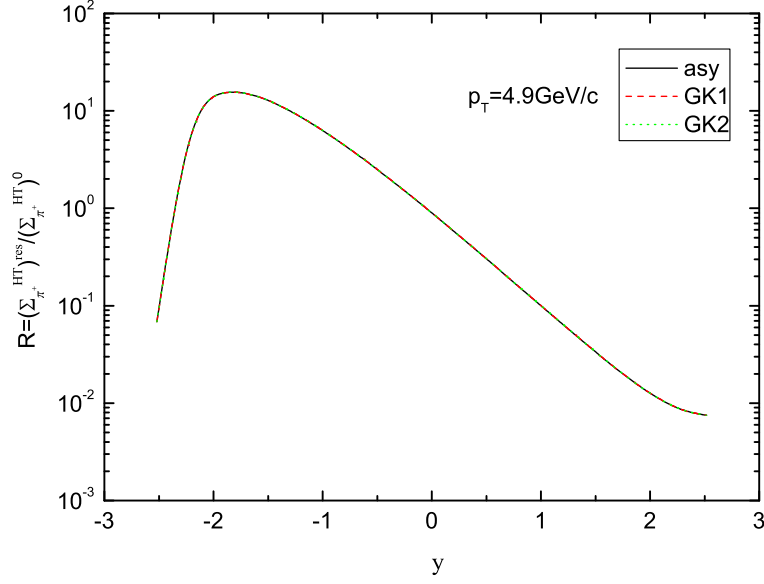


FIG. 6: Ratio $R = (\Sigma_{\pi^+}^{HT})^{res}/(\Sigma_{\pi^+}^{HT})^0$, as a function of the y rapidity of the pion at the transverse momentum of the pion $p_T = 4.9 \text{ GeV}/c$, at the c.m. energy $\sqrt{s} = 62.4 \text{ GeV}$.

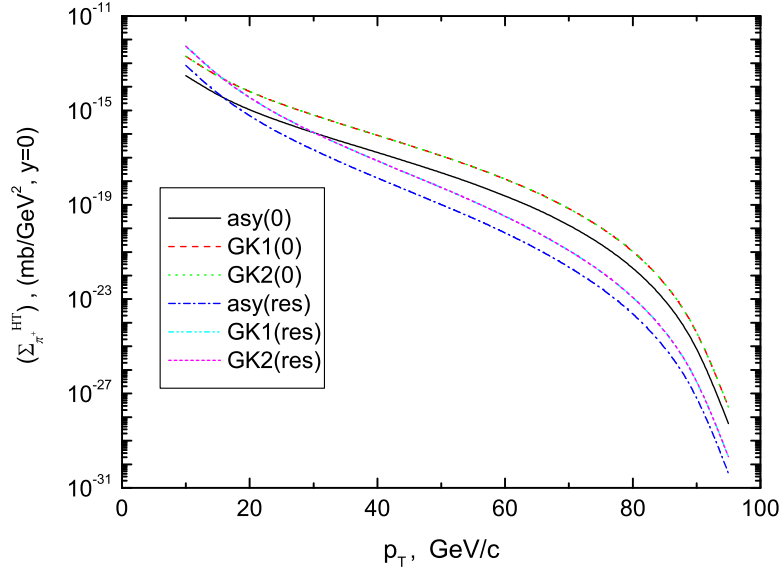


FIG. 7: Higher-twist π^+ production cross section $(\Sigma_{\pi^+}^{HT})$ as a function of the p_T transverse momentum of the pion at the c.m. energy $\sqrt{s} = 200 \text{ GeV}$.

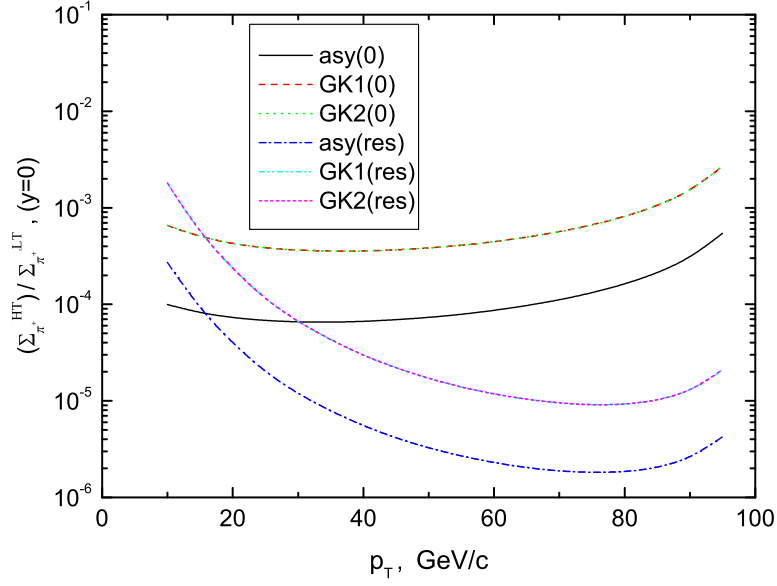


FIG. 8: Ratio $(\Sigma_{\pi^+}^{HT})/\Sigma_{\pi^+}^{LT}$, as a function of the p_T transverse momentum of the pion at the c.m.energy $\sqrt{s} = 200 \text{ GeV}$.

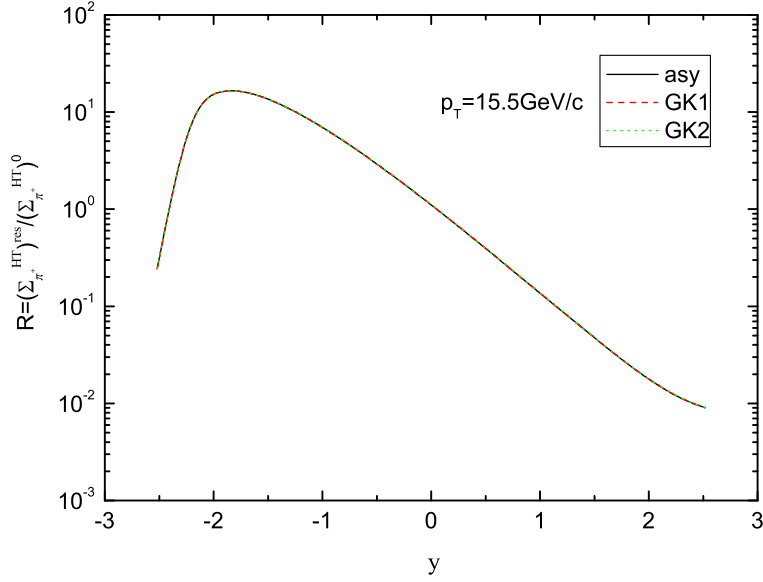


FIG. 9: Ratio $R = (\Sigma_{\pi^+}^{HT})^{res}/(\Sigma_{\pi^+}^{HT})^0$, as a function of the y rapidity of the pion at the transverse momentum of the pion $p_T = 15.5 \text{ GeV}/c$, at the c.m. energy $\sqrt{s} = 200 \text{ GeV}$.